Synthesis, characterization, X-ray structure, DNA binding, antioxidant and docking study of new organotin(IV) complexes

Shaista Ramzan [a, b], Shahnaz Rahim[c], Syed Tasleem Hussain[a], Katherine. B. Holt [b], Jeremy Karl Cockcroft [b], Niaz Muhammad [c], Zia-ur-Rehman [d], Asif Nawaz [a], Shaukat Shujah [a*]

[a] Department of Chemistry, Kohat University of Science and Technology, Kohat 26000, Pakistan

[b] Department of Chemistry, Christopher Ingold Laboratory, University College London WC1H0AJ UK

[c] Department of Chemistry, Abdul Wali Khan University, Mardan, Pakistan

[d] Department of Chemistry, Quaid-i-Azam University, Islamabad 45320, Pakistan

*Corresponding author: Shaukat Shujah

Department of Chemistry, Kohat University of Science and Technology, Kohat 26000, Pakistan.

Email address: dr.shaukat@kust.edu.pk (Shaukat Shujah)

Abstract

Four new diorganotin(IV) complexes including Me_2SnL(**1**), Bu_2SnL(**2**), Ph_2SnL(**3**) and Oct_2SnL(**4**), were synthesized by reacting R_2SnCl_2 (where, R= Me, Bu, Ph, Oct) with N'-(3,5-dichloro-2-hydroxybenzylidene)-2-phenylacetohydrazide **H_2L**. The synthesized ligand and complexes were structurally characterized by various techniques, including FTIR, ^{1}H and ^{13}C-NMR, and mass spectrometry. The data suggested that tin-Oxygen and tin-Nitrogen bonds are formed during complex formation, confirming the coordination of ligand with dialkyltin(IV) moieties and the presence of penta-coordinated structures. The single crystal x-ray study was performed to confirm the molecular structure of complex **1**, which revealed that the molecular structure is distorted toward square pyramidal geometry. The compound-DNA interaction was investigated via spectroscopic, electrochemical, and molecular docking studies, the mode of interaction found in all cases was intercalative in nature. The complex **3** showed the highest binding ability with SS-DNA ($1.93x10^5$ M^{-1}). The data obtained for DNA interaction studies from theoretical calculation via docking studies matches well with that observed from spectroscopic and electrochemical analysis. Electrochemical and thermodynamic parameters, including diffusion coefficient, ΔH, ΔG, and ΔS, were also calculated. The DPPH antioxidant results showed that complex **2** is an active antioxidant.

KEYWORDS

diorganotin(IV) complexes, crystal structure, DNA-binding, electrochemical assay, DPPH antioxidant activity, molecular docking

1. INTRODUCTION

Researchers from last few decades, have been interested in diorganotin(IV) compounds, due to their diverse structures and vast range of uses. In recent era the biological and pharmacological activities of organotin(IV) compounds, as anti-diabetic,[1] anticancer,[2,3] antifungal,[4] antileishmanial,[5] and antibacterial drugs[6] have roused attention. The coordination number, oxidation state of metal atoms, thermodynamic and kinetic features of these complexes influence their biological function. Furthermore, the groups immediately attached to the tin atom not only bestow distinctive medicinal properties to these compounds by changing their solubility in non-aqueous solvents,[7] but they also perform a vital role in the transport of these compounds to specific targets.[6] The nature and amount of organic groups (alkyl or aryl) in organotin(IV) compounds affect their action.[8,9]

Scientists are currently concentrating their efforts on medications that target DNA as their primary target.[10] The study of drug-DNA interactions is critical for developing and manufacturing new DNA-targeted medicines, and their efficacy is determined by the mechanism and affinity of binding.[11,12] Recognizing DNA binders involves a variety of interacting factors, including electrostatic contact, binding with minor and major grooves, and intercalation between neighbouring base pairs.[13,14] Different techniques are being used for drug-DNA interaction including, Electrochemical, UV-visible spectroscopy, circular dichroism $(CD)^2$ spectroscopy, fluorescence spectroscopy etc.[15-18]

Several organotin compounds have been found to relieve the oxidative stress of body by scavenging the free radicals. Antioxidant agents with enhanced medications are also in high demand just like anticancer medications. Various organotin(IV) complexes have been reported in literature, that showed good antimicrobial, anticancer and antioxidant potentials.

Keeping in view the rising demand for compounds which can target DNA, we have synthesized N'-(3,5-dichloro-2-hydroxybenzylidene)2-phenylacetohydrazide and its diorganotin(IV)

complexes (**1-4**). The structural determination of these compounds was done by using IR, ^{1}H and ^{13}C NMR spectroscopies, mass spectrometery and single-crystal XRD. Because tin-based complexes have a great affinity for DNA, so to examine compound-DNA interaction docking studies were also carried out. Following theoretical investigations via molecular docking, compound-DNA interaction was also examined using: electronic absorption spectroscopy, and electrochemical techniques including (CV) cyclic voltammetry, (DPV) differential pulse voltammetry, and (SWV) square wave voltammetry. Furthermore, the antioxidant activity of synthesized ligand (**H_2L**) and complexes (**1-4**) was also carried out using DPPH assay.

2. EXPERIMENTAL SECTION

2.1. Reagents and Chemicals

The reagents including phenylacetic hydrazide, 3,5-Dichlorosalicylaldehyde, 2,2-diphenyl-1-picrylhydrazyl, dimethyltin dichloride, diphenyltin dichloride, dibutyltin dichloride and dioctyltin oxide have been purchased from Alfa Aesar (Thermo Fisher Scientific, Germany). The solvents of analytical grade were purchased from Sigma-Aldrich (Germany), which includes DMSO, chloroform, toluene, ethanol, n-hexane and used without purification. Sodium salt of salmon sperm double strand DNA (SS-DNA) was purchased from Sigma-Aldrich (Merck, Germany).

2.2. Instrumental measurements

The electronic spectra were attained using (AE-S90) AELAB spectrophotometer. The electrochemical parameters were obtained using EmStat2 – PalmSens, (Netherland) and the voltammogram were resolved using software PSTrace5.8. Melting points were determined using melting point instrument (model; AI-5741, i-therm). The IR spectra of the compounds were obtained using a Bruker Alpha II instrument in range 4000-400 cm^{-1}. The nuclear magnetic spectra ^{1}H and ^{13}C of synthesized compounds were obtained in DMSO-d_6 / $CDCl_3$ solvent on a Bruker Advance 300 MHz-spectrometer and TMS (tetramethyl silane) is used as a reference. Mass spectra

were obtained using ASAP-HESI-Q Exactive Plus mass-spectrometer. Crystal analysis was done using a SuperNova Dual Source Single Crystal Diffractometer (Mo X-ray source).

2.3. Synthesis methods

2.3.1. Synthesis of N'-(3,5-dichloro-2-hydroxybenzylidene)-2-phenylacetohydrazide (**H_2L**)

N'-(3,5-dichloro-2-hydroxybenzylidene)-2-phenylacetohydrazide was prepared by mixing equi-molar amounts of Phenylacetic hydrazide (0.006 mol) and 3,5-dichlorosalicylaldehyde (0.006 mol) with continuous stirring at room temperature (25 ± 1 °C) for 2-3 h (Scheme 1). Pale white cotton like precipitate was formed in the flask which were filtered and dried to yield pale white solid.[19]

Yield 96%, M.p.: 230-232 °C. Mol. Wt.: 323.17 (323.03). Anal. Calc. (%) for ($C_{15}H_{12}Cl_2N_2O_2$); Calc. (Found) C, 54.75 (54.05); H, 3.74 (3.54); N, 8.67 (8.70). ESI-MS, m/z (%): $[C_{15}H_{12}Cl_2N_2O_2]^+$ 323.03 (8.02), $[C_7H_5Cl_2N_2O]^+$ 204.99 (28.41), $[C_7H_4Cl_2NO]^+$ 187.96 (100), $[C_9H_9N_2O]^+$ 160.96 (4.55), $[C_8H_8NO]^+$ 134.06 (13.68), $[C_8H_{10}]^+$ 106.07 (10.45). FTIR (cm^{-1}): 3190 m *ν*(NH), 3067 m *ν*(OH), 1763 s *ν*(C=O), 1075 m ν(N-N), 1660 s *ν*(C=N). ^{1}H NMR (ppm): H-4: 7.65 [s, ^{1}H, phenyl], H-6: 7.64 [s, ^{1}H, phenyl], H-7: 8.35 [s, ^{1}H, CH=N], H-9: 3.97 [s, 2H, -CH_2], H-11-15: 7.29-7.60 [m, 5H, phenyl], NH: 12.28 [s, ^{1}H, N-H], O-H: 12.21 [s, ^{1}H, O-H]. ^{13}C NMR (ppm): C-7: 145.97 [HC=N], C-8: 165.82 [CONH], C-1-6: 121.43, 152.15, 122.92, 130.22, 128.27, 128.43 [Ph-C], C-9: 40.78 [CH_2], C-10-15: 135.12, 129.42, 128.18, 126.79 [Ph-C].

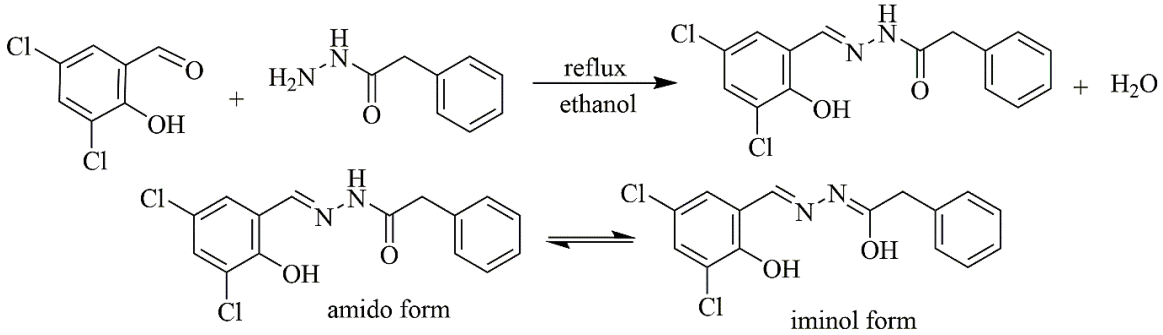

SCHEME 1 Synthesis of N'-(3,5-dichloro-2-hydroxybenzylidene)-2-phenylacetohydrazide

H_2L

2.3.2. Synthesis of Complexes (1-4)

N'-(3,5-dichloro-2-oxidobenzylidene)-2-phenylacetohydrazide (0.0015 mol) was taken in a flask (100 mL) and toluene (50 mL) was added with constant mixing at ambient temperature. To this mixture, triethylamine (0.003 mol) was added and agitated for 15 min. After 15 min the R_2SnCl_2 (0.0015 mol) solution in toluene was poured to above solution and the resulting solution was stirred for 5 h at room temperature. The toluene was removed using rotary-evaporator. Resulting yellowish solid product was dried at room temperature and recrystallized from n-hexane:chloroform mixture (1:4).[20] The synthesis of the diorganotin(IV) complexes (**1-3**) is illustrated in Scheme 2a as a general chemical equation, whereas Scheme 3 depicts the numbering patterns of H_2L and the organotin groups linked to it for NMR interpretation.

Dimethyltin(IV)-N'-[(3,5-dichloro-2-oxidobenzylidene)-2-phenylacetohydrazide] (1)

Yield 82%, M.p.: 155-157 °C. Mol. Wt.: 469.94 (469.97). Anal. Calc. (%) for ($C_{17}H_{16}Cl_2N_2O_2Sn$): Cal. (Found) C, 42.45 (42.20); H, 2.93 (2.90), N, 6.06 (5.98). ESI-MS, m/z (%): $[C_{17}H_{18}Cl_2N_2O_2Sn]^+$ 470.96 (100), $[C_{17}H_{18}Cl_2N_2O_2Sn]^+$ 469.97 (37.12), $[C_{10}H_{11}C_{l2}N_2O_2Sn]^+$ 380.92 (7.98), $[C_9H_9N_2O]^+$ 161.07 (5), $[C_2H_6Sn]^+$ 148.04 (10.39), $[C_8H_{10}]^+$ 107.05 (15.12). FT-IR (4000-400 cm^{-1}): 1601 s ν(C=N), 1076 m ν(N-N), 528 m ν(Sn–O), 454 w ν(Sn–N). ^{1}H NMR (ppm): H-4: 7.42 [d, ^{1}H, phenyl, $^3J_{H\text{-}H}$ = 5.2], H-6: 7.01 [d, ^{1}H, phenyl, $^3J_{H\text{-}H}$ = 2.5], H-7: 8.53 [s, ^{1}H, CH=N], $^3J(^{119}Sn\text{-}^1H)$ = 42 Hz, H-9: 3.61 [s, 2H, -CH_2], H-11-15: 7.24–7.32 [m, 5H, phenyl], H-α: 0.78 [s, 6H, 2CH_3], $^2J(^{119/117}Sn\text{-}^1H)$ = 78 Hz. ^{13}C NMR (ppm): C-7: 159.89 [HC=N], C-8: 175.17 [CO=N], C-1-6: 117.65, 159.81, 120.74, 134.23, 126.94, 129.03 [Ph-C], C-9: 41.20 [CH_2], C-10-15: 136.15, 131.11, 128.64, 126.75 [Ph-C], C-α: 1.89 $^1J[^{119/117}Sn\text{-}^{13}C]$ = 402 Hz.

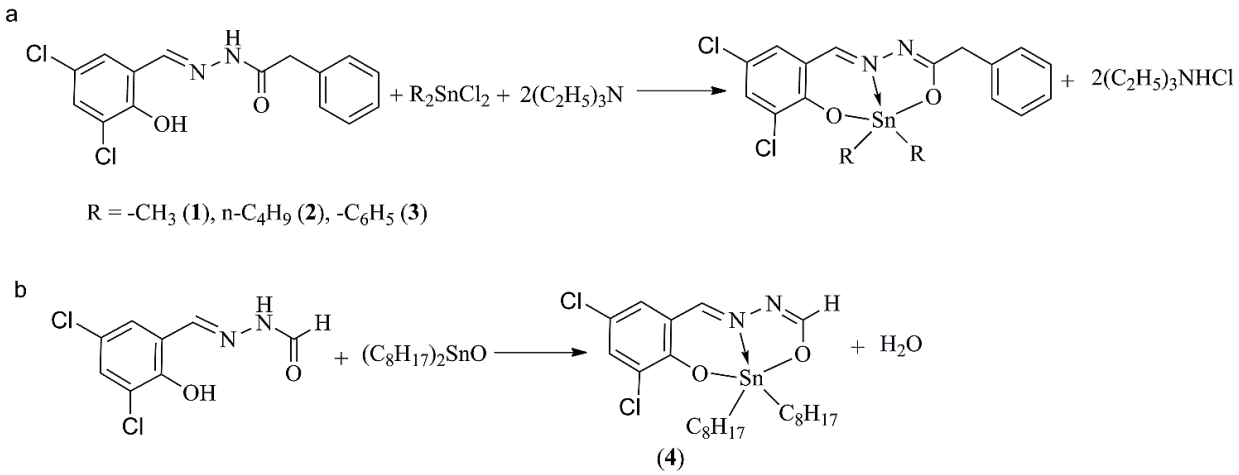

SCHEME 2 Synthesis of diorganotin(IV) complexes (**1-4**)

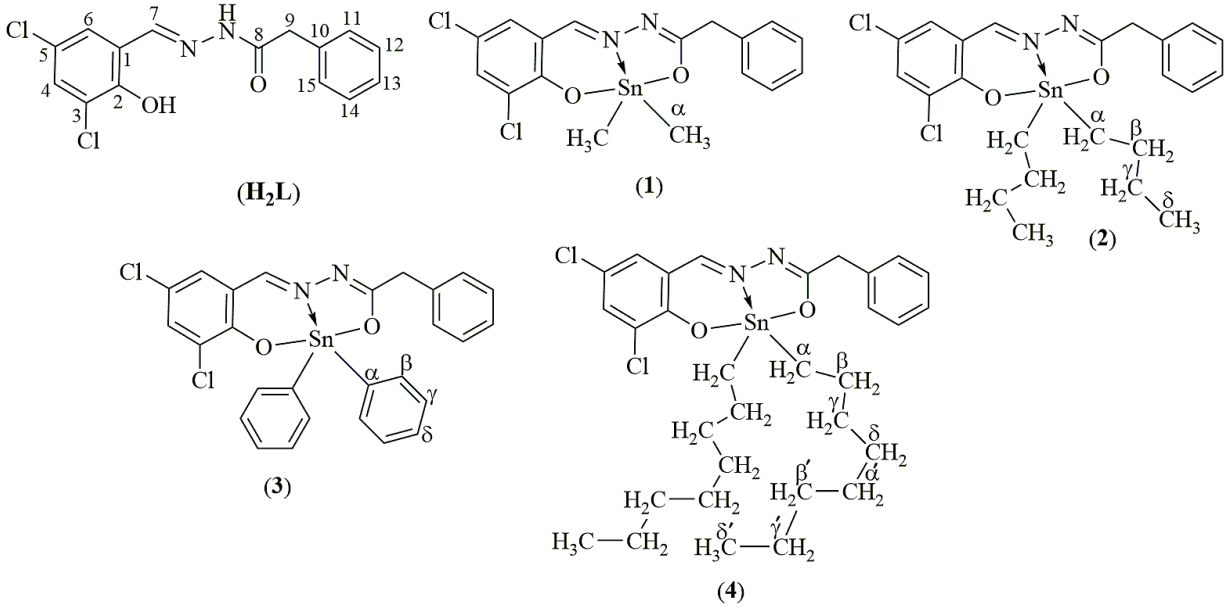

SCHEME 3 Numbering scheme of ligand (**H_2L)** and organotin(IV) complexes (**1-4**)

Dibutyltin(IV)-N'-[(3,5-dichloro-2-oxidobenzylidene)-2-phenylacetohydrazide] (2)

Yield 80%, viscous liquid, Mol. Wt.: 554.10 (554.06). Anal. Calc. (%) for ($C_{23}H_{28}Cl_2N_2O_2Sn$): Cal. (Found) C, 49.86 (49.70); H, 5.09 (4.88); N, 5.06 (5.00). ESI-MS, m/z (%): $[C_{23}H_{30}Cl_2N_2O_2Sn]^+$ 554.06 (72.06), $[C_{15}H_{22}Cl_2N_2OSn]^+$ 438.92 (100), $[C_7H_3Cl_2NOSn]^+$ 305.87 (8.50), $[C_8H_{10}N_2OSn]^+$ 266.97 (14.50), $[C_4H_9Sn]^+$ 175.97 (2.44), $[C_8H_9NO]$ 134.90 (12.37). FT-

IR (4000-400 cm^{-1}): 1600 s *ν*(C=N), 1074 m ν(N-N), 511 m *ν*(Sn–O), 453 w *ν*(Sn–N). ^{1}H NMR (ppm): H-4: 7.41 [d, ^{1}H, phenyl, $^{3}J_{H-H}$ = 2.6], H-6: 7.05 [d, ^{1}H, phenyl, $^{3}J_{H-H}$ = 2.5], H-7: 8.52 [s, ^{1}H, CH=N], $^{3}J(^{119}Sn-^{1}H)$ = 40 Hz, H-9: 3.60 [s, 2H, -CH_2], H-11-15: 7.23–7.32 [m, 5H, phenyl], H-α: 1.58 [m, 4H, 2CH_2], H-β: 1.42-1.53 [m, 4H, 2CH_2], H-γ: 1.23-1.31 [q, 4H, 2CH_2, $^{3}J_{H-H}$ = 6.9], H-δ: 0.81 [t, 6H, 2CH_3, $^{3}J_{H-H}$ = 7.2]. ^{13}C NMR (ppm): C-7: 160.37 [HC=N], C-8: 175.49 [CO=N], C-1-6: 117.70, 159.46, 120.35, 134.04, 126.89, 129.12 [Ph-C], C-9: 41.35 [CH_2], C-10-15: 136.31, 131.04, 128.55, 126.77 [Ph-C], C-α: 26.68, C-β: 26.50, C-γ: 22.55, C-δ: 13.64.

Diphenyltin(IV)-N'-[(3,5-dichloro-2-oxidobenzylidene)-2-phenylacetohydrazide] (3)

Yield 78%, M.p.: 135-137 °C, Mol. Wt.: 594.08. Anal. Calc. (%) for ($C_{27}H_{20}Cl_2N_2O_2Sn$): Cal. (Found) C, 54.59 (54.50); H, 3.39 (3.30); N, 4.72 (4.70). FT-IR (4000-400 cm^{-1}): 1599 s *ν*(C=N), 1074 m ν(N-N), 534 m *ν*(Sn–O), 447 w *ν*(Sn–N). ^{1}H-NMR (ppm): H-4: 7.68 [d, ^{1}H, phenyl, $^{3}J_{H-H}$ = 7.5], H-6: 7.65 [d, ^{1}H, phenyl, $^{3}J_{H-H}$ = 1.6], H-7: 8.52 [s, ^{1}H, CH=N], $^{3}J(^{119}Sn-^{1}H)$ = 49 Hz, H-9: 3.74 [s, 2H, -CH_2], H-11-15: 7.30–7.33 [m, 5H, phenyl], H-β: 7.65-7.68 [m, 4H], H-γ: 7.29-7.45 [m, 4H], H-δ: 7.29-7.45 [m, 4H]. ^{13}C-NMR (ppm): C-7: 160.17 [HC=N], C-8: 174.41 [CO=N], C-1-6: 95.25, 159.82, 117.78, 131.30, 127.07, 127.35 [Ph-C], C-9: 41.52 [CH_2], C-10-15: 136.21, 130.89, 129.51, 121.26 [Ph-C], C-α: 137.94, C-β: 134.35, C-γ: 129.11, C-δ: 128.63.

Dioctyltin(IV)-N'-[(3,5-dichloro-2-oxidobenzylidene)-2-phenylacetohydrazide] (4)

Equimolar amounts (0.0015 mol) of N'-(3,5-dichloro-2-oxidobenzylidene)-2 phenylaceto hydrazide and dioctyltin(IV) oxide were mixed in 100 mL toluene. The resultant yellowish solution was refluxed for 3-4 hr until the solution became clear. Using the Dean and Stark Apparatus, water formed as a by-product during reaction water was removed. After removing solvent the final product obtained was oily in nature (Scheme 2b).

Yield 77%, M.p.: 145-146 °C. Mol. Wt.: 666.32. Anal. Calc. (%) for ($C_{31}H_{44}Cl_2N_2O_2Sn$): Cal. (Found) C, 55.88 (55.21); H, 6.66 (6.53); N, 4.20 (4.31). FT-IR (4000-400 cm^{-1}): 1609 s *ν*(C=N),

1076 m ν(N-N), 532 m *ν*(Sn–O), 452 w *ν*(Sn–N). ^{1}H NMR (ppm): H-4: 7.41 [d, ^{1}H, phenyl, $^{3}J_{H\text{-}H}$ = 2.6], H-6: 7.00 [d, ^{1}H, phenyl, $^{3}J_{H\text{-}H}$ = 2.6], H-7: 8.51 [s, ^{1}H, CH=N], $^{3}J(^{119}\text{Sn-}^{1}\text{H})$ = 40 Hz, H-9: 3.60 [s, 2H, -CH_2], H-11-15: 7.23–7.34 [m, 5H, phenyl], H-α: 1.52-1.54 [bs, 4H, 2CH_2], H-β: 1.42-1.47 [m, 4H, 2CH_2], H-γ-γ': 1.19-1.25 [bs, 20H, 2CH_2 $CH_2CH_2CH_2$ CH_2], H-δ': 0.86 [t, 6H, 2CH_3, $^{3}J_{H\text{-}H}$ = 7.0]. ^{13}C NMR (ppm): C-7: 160.37 [HC=N], C-8: 175.47 [CO=N], C-1-6: 120.35, 159.41, 117.73, 134.02, 126.88, 129.11 [Ph-C], C-9: 41.34 [CH_2], C-10-15: 136.32, 131.02, 128.55, 126.80 [Ph-C], C-α: 22.77, C-β: 24.57, C-γ: 33.48, C-δ: 29.14, C-α': 29.26, C-β': 31.95, C-γ': 23.05, C-δ': 14.23.

2.4. DNA-Interaction studies

2.4.1. Spectroscopic studies

The electronic spectra were measured on a (AE-S90) AELAB spectrophotometer. 4 mg of SS-DNA (Salmon sperm, double strand) was dissolved in 40 mL of double distilled water, to produce SS-DNA solution and was stirred overnight before storing it at [4 °C]. The purity and DNA concentration of the above solution was determined using the previously described method[21,22] and was found to be 2×10^{-4} M. The drug was titrated against SS-DNA solution by adding different concentrations of DNA solution (5-25 M) to a constant concentration (0.1 mM) of synthesized ligand (H_2L) and diorganotin(IV) complex (**1-4**) solution. The solutions were allowed to stand for 5-10 minutes and titration curve was obtained using UV-vis spectrophotometer.

2.4.2. Electrochemical assay

To find out general electrochemical properties and drug-DNA interaction model, CV, DPV and SWV techniques were applied. Voltammograms of synthesized compounds were obtained in 70% DMSO, using three electrode cell and for supporting electrolyte TBAP (tetrabutylammonium perchlorate) was used.

The glassy carbon (GC) electrode was used as working electrode, with surface area (A) of 0.03 cm^2, Pt wire as a counter electrode, and (Ag/AgCl) saturated silver/silver chloride was used as a

reference electrode. The electrodes were cleaned and solution was pre-treated with Argon before using, as reported in literature.[23] For CV technique scan rate (ν) of (100 mV/s) and E step (10 mV) was used. The DPV voltammogram were attained at conditions: 1 mV Potential increment, 50 ms pulse width and 100 mVs^{-1} scan rate (ν). SWV voltammogram were attained at conditions: 10 Hz frequency, 2 mV pulse amplitude, and 5 mV potential increment.

2.6. DNA Interaction studies by molecular docking

SS-DNA X-ray crystallographic structure was used for docking analysis to locate the possible molecular interactions of the newly prepared compounds. The structures of the synthesized compounds were drawn by using chemdraw software. The crystal structure of the SS- DNA was retrieved from PDB database [1BNA [www.rcsb.org/pdb]. The molecular Operating Environment software was used with default parameters, i.e., Placement: Triangle Matcher, London dG to calculate the free energy of binding in a target structure at a particular position as scoring function 1 and 2 with the generation of 10 confirmations of each ligand to better fit within the binding pocket. The top ranked confirmation of each molecule was used for further analysis.

2.7. Antioxidant assay

The (2,2-diphenyl-1-picrylhydrazyl), DPPH radical antioxidant activity of the ligand (**H_2L**) and its organotin(IV) complexes (**1–4**), was evaluated using a spectrophotometer to measure the variation in DPPH absorbance at (517 nm).[24-26] The activity of the synthesize compounds were tested for varied concentrations of ligand and complexes (12.5, 25, 50, 100, 200 µg/mL), in DMSO. The procedure adopted for the study is reported in literature.[26] The standard used for comparison of antioxidant activity was ascorbic acid. Using following equation (1), % inhibition of the compounds was calculated.

$$(\%)\ \text{inhibition} = [\ (A - A_t)\ /A] \times 100 \qquad (1)$$

A = absorption value of the control, where A_t = absorption of the test samples.

The above graph was used to derive the IC_{50} values of the tested compounds.

3. RESULTS AND DISCUSSIONS

3.1. FTIR

In FT-IR spectrum of ligand **H_2L**, its characteristic bands at 3197 cm^{-1}, 3047 cm^{-1} and 1763 cm^{-1}, were observed owing to the stretching vibrations of (N-H), (OH) and (C=O) groups in the ligand, respectively (Figure S1). All these bands disappear in the IR spectra of complexes due to deprotonation and formation of new bonds with tin. In diorganotin(IV) complexes (**1-4**), the band at 1660 cm^{-1}, characteristic of azomethine group ν(C=N) was displaced to lesser values 1598-1609 cm^{-1}, signifying it's coordination with the Sn atom.[26-27] The ν(C-O) band at (1283 cm^{-1}) in ligand H_2L was shifted to higher values (1296-1306 cm^{-1}) in diorganotin(IV) complexes (**1-4**), indicationg it's coordination with the Sn atom (Figures S2-S5). New bands were also detected in the region of 604-607 cm^{-1} and 447-463 cm^{-1} allocated to ν(Sn-O) and ν(Sn-N), respectively for all complexes (**1-4**).[26] The emergence of these bands proved that the organotin(IV) complexes had been synthesised.[20]

3.2. ^{1}H and ^{13}C NMR

The ^{1}H and ^{13}C NMR spectra were obtained using DMSO-d_6/$CDCl_3$ as a solvent (Figures S6-S15). The chemical shifts (ppm) values obtained in both NMR were found to be in the anticipated range. In synthesized complexes (**1-4**), coordination of tin with nitrogen atom was proved by the presence of Sn satellite. These peaks were appeared owing to $^{3}J(^{119}Sn\text{-}^{1}H)$ spin–spin coupling (^{3}J = 40–49 Hz).[28-29] For complex **1** the $^{2}J(^{1}H–^{119}Sn)$ coupling constant value obtained is 78 Hz, that indicated penta-coordinated geometry of the complex.[30-31] The angle of C-Sn-C is determined using Lockhart's equation and is found to be 138.40°. Thus, it confirmed that in solution the Sn atom have five coordinates. In all synthesized complexes (**1-4**), signals detected in ^{13}C-NMR are in conformation with the anticipated composition.[20]

3.3. Single crystal x-ray analysis of complex (1)

As observed from crystal data presented in Table 1 complex (**1**) belong to monoclinic crystal system and space group P21/c. The selected bond lengths and angles are given in Table 2. The molecular diagram of complex (**1)** is given in Figure 1. The crystallographic structure shows that ligand is tridentate in nature and is bonded to dimethyltin(IV) moiety via ONO atoms. Due to formation of five and six membered rings during complexation, the ligand become non-planar due to steric effect. The five membered ring in complex (**1)** consists of Sn1, O2, C8, N2, N1 atoms and Sn1, N1, Sn1, O1, C1, C6 atoms form six membered rings. The value of τ is used to characterize the geometry around tin atom, where $\tau = (\beta - \alpha)/60$, where β is the largest and α is the second largest basal angle. For complex (**1**) (β = O1-Sn1-O2 = 154.87°), and (α = C10-Sn1-C9 =131.21°) so the τ value (0.38) obtained, indicated a distorted square-pyramidal geometry with two methyl carbons and two enolic oxygens in the equatorial positions and the azomethane nitrogen (C=N) at the apical position. The observed bond lengths of the Sn-O1 and Sn-O2 are (2.092(16) and 2.4121(16) Å) respectively, which are lower than the sum of van der Waals radii of Sn and O (3.68 Å). The bond angles for O1-Sn-N1 (82.37°) and O2-Sn-N1 (72.62°) are obtained. The bond angles for C10-Sn-C9 (131.21° (12)) deviate significantly from the linear value (180°) and the angle calculated from $^{2}J(^{119}\text{Sn-}^{1}\text{H})$ (138.40°) by Lockhart equation.[31] A strong bond formed between the Sn(1) and azomethine N(2) as observed from the bond distance (2.178(18)Å) which is equivalent to the sum of the covalent radii of Sn and N (2.15 Å) and lower than the sum of the van der Waals radii (3.75 Å). All the bond distances and bond angles are within normal ranges, which are comparable with the corresponding values reported in the literature. In the packing diagram of complex **1** the two molecules are connected together via intermolecular Cl(1)---H(7) hydrogen bonds, and form a wavy structure Figures 2,3.

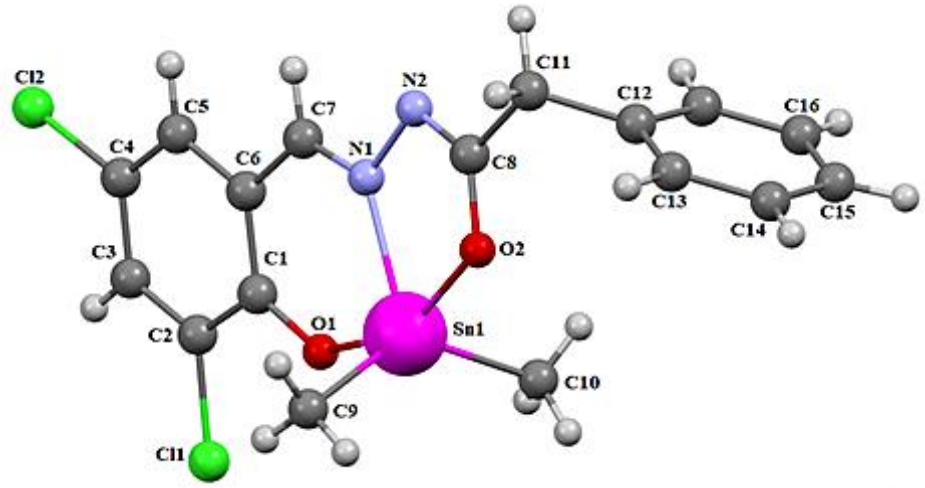

FIGURE 1 Molecular structure of complex **1**

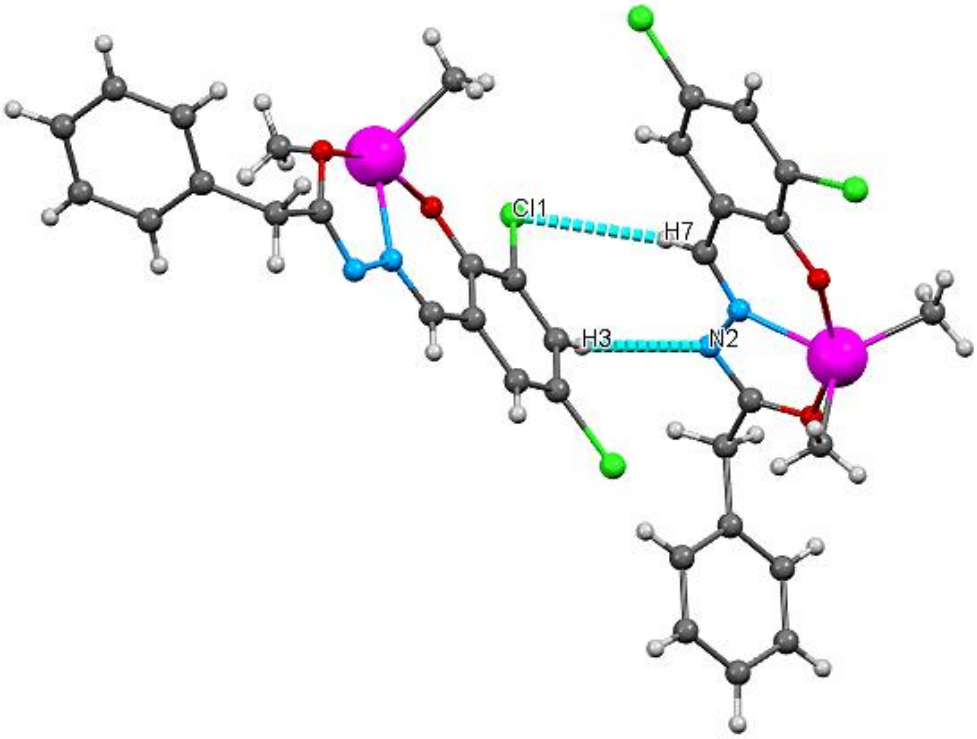

FIGURE 2 Dimeric structure of complex **1**, molecules connected via Cl(1)···H(7) and N(2)···H(3) interaction.

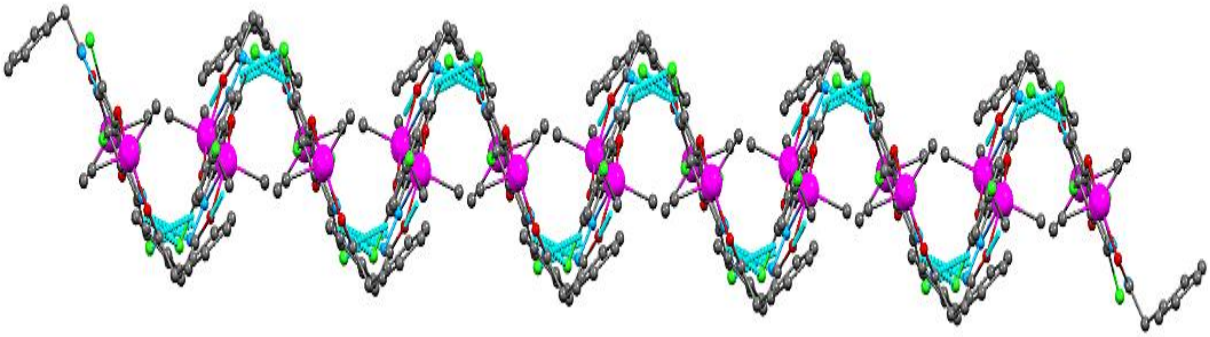

FIGURE 3 Wavy layered packing diagram of complex **1**

TABLE 1 Structural parameters and crystal data for complex **1**

Parameters	**Complex 1**
Empirical formula	$C_{17}H_{16}Cl_2N_2O_2Sn$
Formula weight	469.91
Crystal system	Monoclinic
Space group	$P2_1/c$
a (Å)	9.0129(3)
b (Å)	10.1263(3)
c (Å)	19.8558(7)
α (°)	90
β (°)	89.860(3)
γ (°)	90
Volume ($Å^3$)	1812.18(10)
Z	4
Crystal habit	Block
Crystal size/mm^3	0.331 × 0.168 × 0.162
Temperature/K	150
P (g/cm^3)	1.722
μ ($mm^{-1)}$	1.716
F(000)	928
Radiation	MoKα (λ = 0.71073)
2Θ range for data collection/°	7.306 to 59.144
Index ranges	$-11 \le h \le 12$, $-13 \le k \le 14$, $-25 \le l \le 26$
Reflections collected	30600
Independent reflections	4720 [R_{int} = 0.0367, R_{sigma} = 0.0262]
Data/restraints/parameters	4720/15/277
Goodness-of-fit on F^2	1.059
Final R indexes [I>=2σ (I)]	R_1 = 0.0276, wR_2 = 0.0596

Final R indexes [all data]	R_1 = 0.0352, wR_2 = 0.0632
Largest diff. peak/hole (e $Å^{-3}$)	0.52/-0.70

TABLE 2 Selected bond lengths (Å) and bond angles (˚) of Complex **1**

Bond lengths of Complex 1			
Sn(1)-O(1)	2.0927(16)	N(1)-N(2)	1.404(3)
Sn(1)-O(2)	2.1428(16)	N(2)-C(8)	1.304(3)
Sn(1)-N(1)	2.1782(18)	N(1)-C(7)	1.294(3)
Sn(1)-C(9)	2.099(3)	C(1)-O(1)	1.310(3)
Sn(1)-C(10)	2.094(3)	C(1)-O(8)	1.286(3)
Bond Angles of Complex 1			
O(1)-Sn(1)-O(2)	154.87(7)	O(2)-Sn(1)-C(10)	94.06(11)
O(1)-Sn(1)-N(1)	82.37(7)	O(2)-Sn(1)-C(9)	94.69(9)
O(1)-Sn(1)-C(9)	97.47(10)	N(1)-Sn(1)-C(9)	113.30(9)
O(1)-Sn(1)-C(10)	94.06(11)	N(1)-Sn(1)-C(10)	115.17(10)
O(2)-Sn(1)-N(1)	72.62(6)	C(10)-Sn(1)-C(9)	131.21(12)
C(8)-N(2)-N(1)	110.72(18)		

3.4. DNA interaction studies

3.4.1. Electronic spectroscopic studies

The absorption spectra of synthesized compounds were obtained by keeping the concentration of the ligand (**H_2L**) and its complexes (**1-4**) constant, at varied concentrations of DNA. The tri-dentate ligand (**H_2L**) showed broad bands of absorption owed to the π-π* (315-355 nm) and n-π* (355-360 nm) energy-levels excitations in the visible region.[20]

The DNA-binding results of ligand (**H_2L**) shows a slight bathochromic shift (**1-4** nm) of the both spectral band with significant hypochromicity in π-π* band and hyperchromic effect n-π* band indicating intercalation as well as groove binding of the ligand (**H_2L**) with the SS-DNA helix (Figure 4).[32] The organotin(IV) complexes (**1-4**) of the ligand (**H_2L**) shows blue shift upto 2-5 nm along with hypochromic effect, indicating the intercalative mode of interaction (Figure 5).[33] In the intercalative mode, intercalated compound's orbital might get attached with the orbital in base pairs of SS-DNA, which results in the decrease of transition energy and peak intensity.[16]

Furthermore, the spectra of ligand (**H_2L**) and complexes (**1-4**) shifts and is defined by one isosbestic point when titrated with DNA (Figure 4,5), as a result, the existence of species apart from free and bound complexes can be eliminated.[34] Presence of the isosbestic point in the spectra, implies that there is an equilibrium between the free drug and DNA adduct.[35]

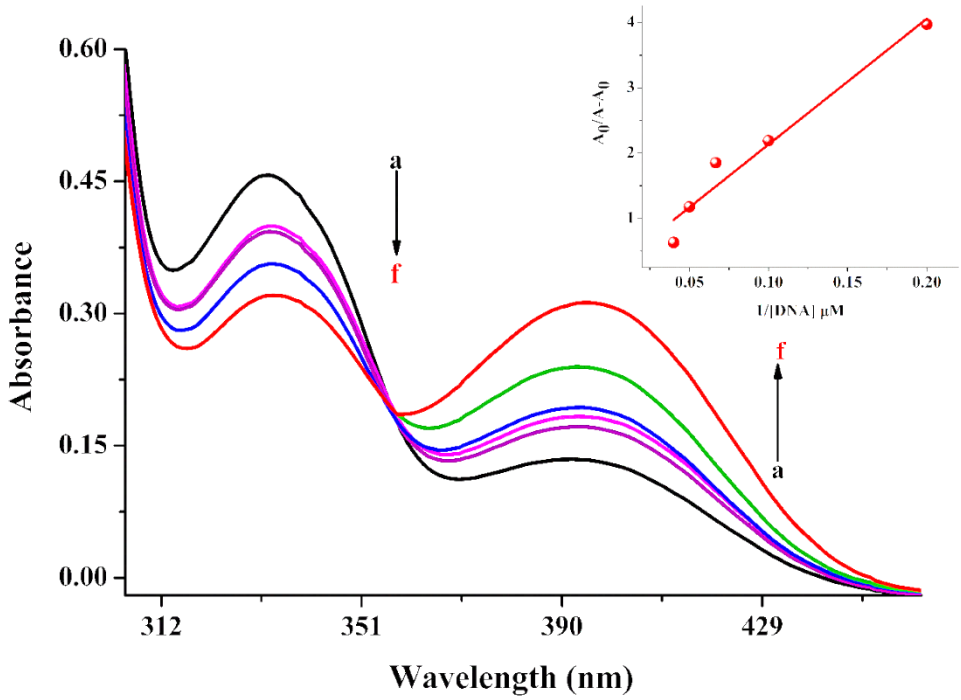

FIGURE 4 Absorption spectrum of 0.1 mM of ligand **H_2L** without (a) and in presence (**b-f**) of (5-25µM) SS-DNA. Inserted plot is $A_o/A\text{-}A_o$ vs. $1/[DNA]$ $(\mu M)^{-1}$.

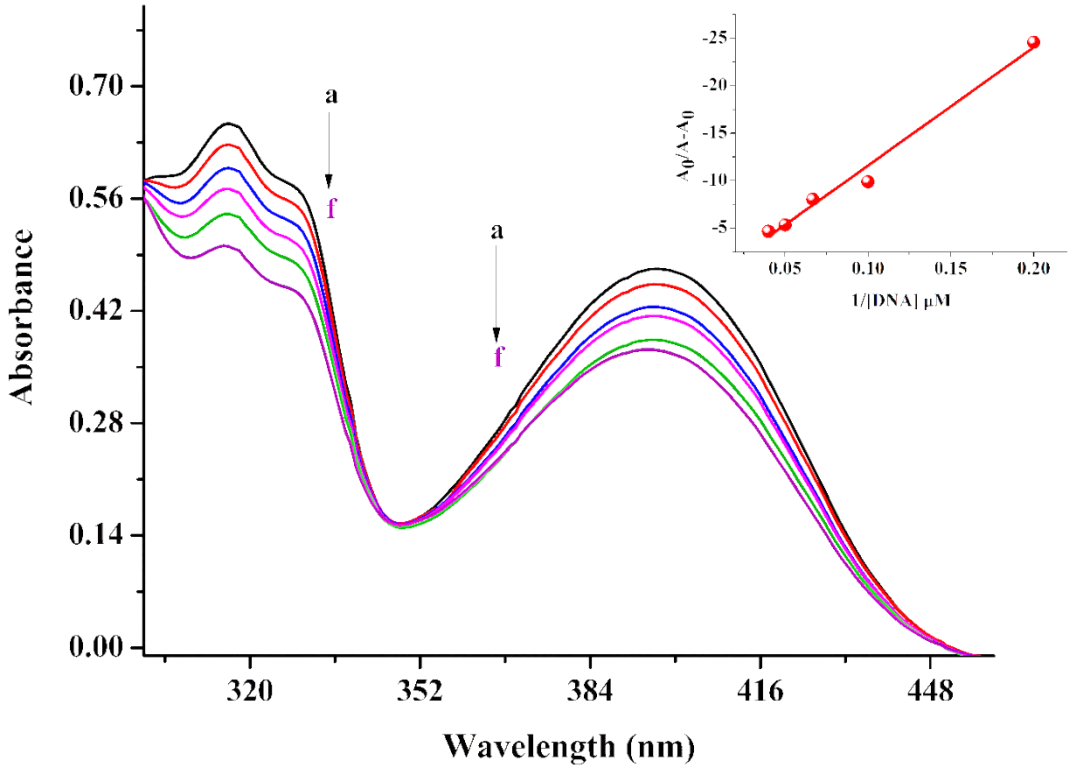

FIGURE 5 Absorption spectrum of 0.1 mM of complex **2** without (**a**) and in the presence (**b-f**) of (5-25μM) SS-DNA. Inserted plot is $A_o/A\text{-}A_o$ vs. 1/[DNA] $(\mu M)^{-1}$.

From the data of variation in peak intensity of all compounds, the binding constant (K_b) value can be calculated using Benesi-Hildebrand equation (eq. 2).[37]

$$\frac{A_0}{A-A_0} = \frac{\varepsilon_G}{\varepsilon_{H-G}-\varepsilon_G} + \frac{\varepsilon_G}{\varepsilon_{H-G}-\varepsilon_G} \times \frac{1}{K_b[DNA]} \qquad (2)$$

A_o and A are the absorption peak of free and complex-DNA adduct and ε_G and $\varepsilon_{H\text{-}G}$ are the molar-extinction coefficients of unbound complex and complex-DNA adducts.

From $A_o/(A\text{-}A_o)$ vs. 1/[DNA] plot, the intercept to slope ratio is used to determine (K_b) binding constant. The observed trend in binding constant values (K_b) for synthesized complexes is **3**>**2**>**4**>**1** at 298 K and **3**>**4**>**2**>**1** at 310 K. Complex **3** showed the highest binding constant value at both temperatures (Table 3).

Using the K_b values, (ΔG) Gibb's free energy, was also calculated using equation (3).[38]

$$\Delta G = -RT \ln K_b \qquad (3)$$

The ΔG° value for the complex-DNA adduct formation is negative as listed in Table 3 indicating spontaneity of the process.

Enthalpy (ΔH) and entropy (ΔS) values were calculated by using equation 4 and 5.

$$-\Delta H = \frac{RT_1T_2 \ln\left(\frac{K_2}{K_1}\right)}{T_2 - T_1} \quad (4)$$

$$\Delta G = \Delta H - T\Delta S \quad (5)$$

The enthalpy (ΔH) value was positive (ΔH > 0) for H_2L and complexes (**1-4**), so the endothermic nature of the reaction is indicated and favoured by positive entropy value (ΔS > 0).[39]

TABLE 3 Thermodynamic data and binding constants of ligand (**H_2L)** and its complexes (**1-4**)

Compounds	T (K)	K_b	ΔG (kJ/mol)	ΔH (kJ)	ΔS (kJ/K)
H_2L	298	1.06E+04	-22.96	24.26	0.16
	310	1.55E+04	-24.87		
1	298	1.30E+04	-23.48	59.69	0.28
	310	6.56E+03	-26.82		
2	298	6.28E+04	-27.37	7.53	0.12
	310	7.20E+03	-28.78		
3	298	1.93E+05	-30.15	9.99	0.13
	310	2.25E+05	-31.77		
4	298	2.35E+04	-24.93	23.06	0.16
	310	3.37E+04	-26.87		

3.4.2. Electrochemical assay

Cyclic voltammetry

The drug-DNA interaction studies of complexes (**1-3**) were also done with CV, in 70% DMSO. The CV of the complexes (**1), (2),** and **(3**) of concentration (3 mM) were taken in the absence of SS-DNA. The peaks were observed around -1.40 V, -1.38 V, -1.32 V, respectively, and credited to the tin reduction from Sn^{+4} to Sn^{+2} state. No peak is observed in the reverse scan for complexes (**1-3**), indicating irreversible nature of the system (Figure 6). The reduction peak in all complexes

is quite broad in nature, and this broadness is due to the overlapping of two reduction peaks, each contributing 1e as directed by equation [E_p-$E_{p/2}$] = 70 mV.[20]

The CV of complexes (**1-3**) solutions were also done after adding varied concentrations of SS-DNA (20-100 μM). During drug-DNA adduct formation various changes in electrochemical signals were observed including decline in cathodic peak current (I) and shifting in the peak potential (E). At 100 μM SS-DNA concentration in complexes (**1-3**) solutions, percentage decline in peak current (I) of 63, 75, 77 observed, respectively and negative shift of 80 mV, 20 mV, 10 mV, in peak potential (E) was also observed, respectively, as mentioned in Figure 6. As reported in literature the reduction in cathodic peak current and negative shift, show intercalative mode of interaction between DNA and complex molecules.[38,40]

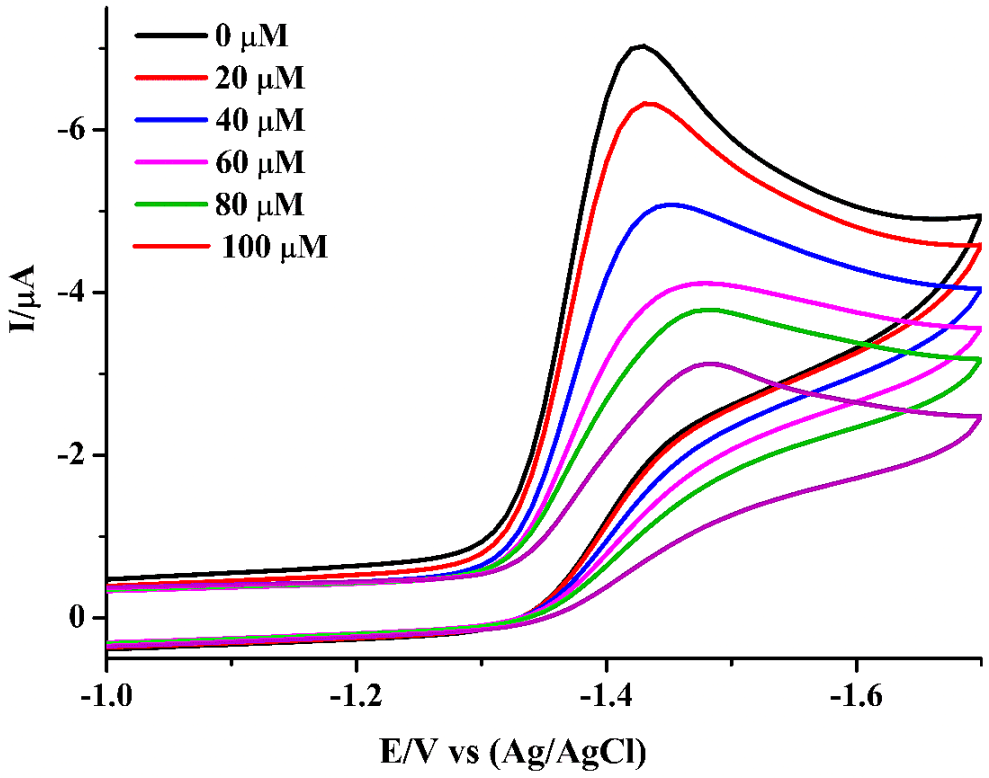

FIGURE 6 Cyclic voltammogram of complex **3** at different concentration (20-100 μM) ssDNA.

Using Randlese Sevcik equation (6) for irreversible process, diffusion coefficient values for complexes (**1-3**) were determined, in presence and absence of SS-DNA.[41,42]

$$Ip = 2.99 \times 10^5\, n\, (\alpha n)^{1/2}\, AC_o^{*}\, D^{1/2}\, \upsilon^{1/2} \qquad (6)$$

Ip is peak current, α is the transfer coefficient ($0.3 < \alpha < 0.7$), n is charge transfer number, A (cm^2) is the electrode's surface area, diffusion coefficient is D ($cm^2\ s^{-1}$), C_o^{*} (mol cm^{-3}) is the of the sample species concentration and υ (V s^{-1}) is the scan rate.

The Ip vs $\nu^{1/2}$ graph was plotted for complexes (**1-3),** with and without the existence of DNA, which were found linear. The primary mass transport to the surface of the electrode for these complexes (**1-3**) is found to be diffusion controlled, results obtained from the linearity of the plot (Figure 7).[43]

The diffusion coefficient of the complexes (**1-3**) without and after addition of SS-DNA was calculated (Table 4) and it is observed that in the existence of DNA, the diffusion of redox species is slower, as evident from the lower diffusion coefficient values of complex. As the free complex bound with DNA to form complex-DNA adduct, its concentration in solution was decreased so decrease in peak currents of cyclic-voltammograms occurs (Figure 6).

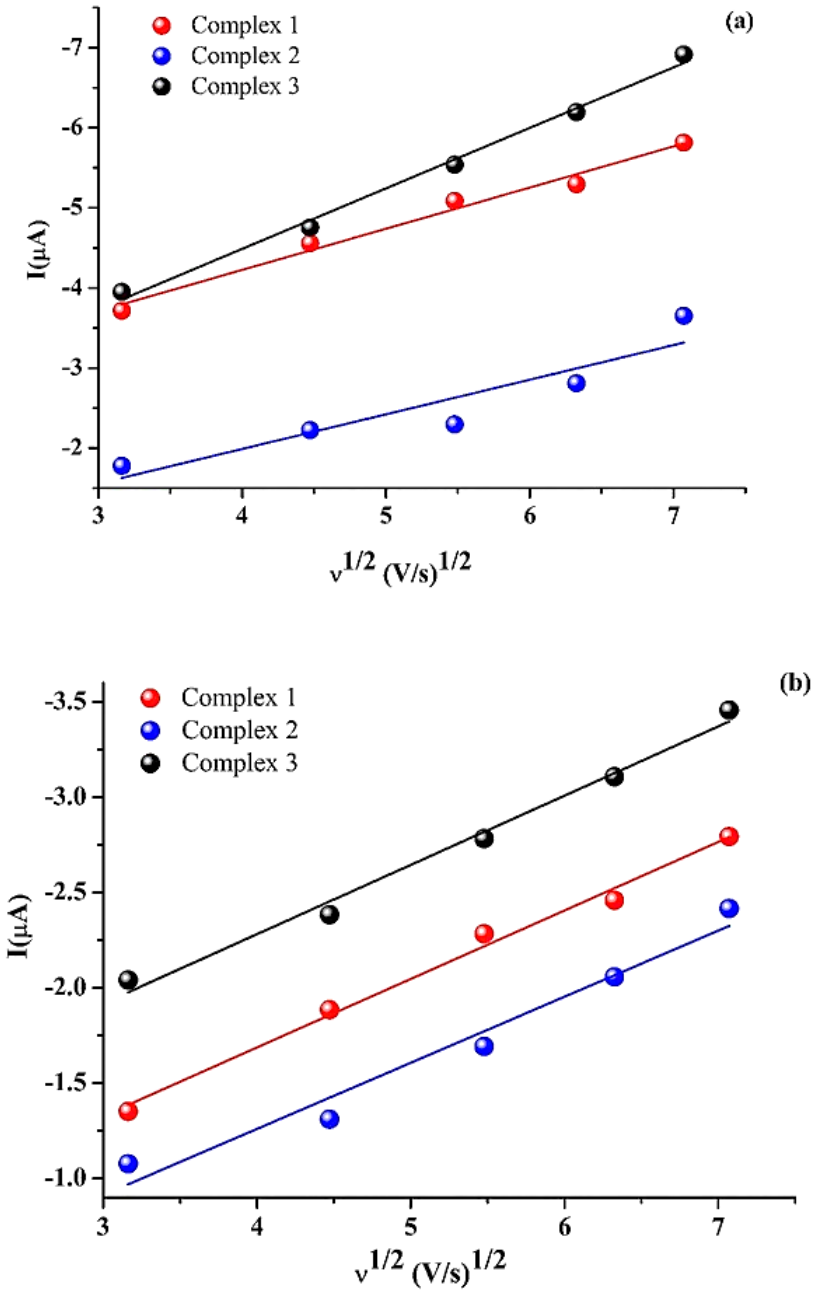

FIGURE 7 Randlese Sevcik plot **(a)** absence of DNA **(b)** Presence of SS-DNA, of complexes (**1-3**).

The stability constant (K) values for Complex-DNA adduct were calculated, using following equation.[44]

$$1/[\mathrm{DNA}] = \frac{\mathrm{K}(1-\mathrm{A})}{(1-\frac{\mathrm{I}}{\mathrm{I_0}})} - \mathrm{K} \qquad (7)$$

The binding constant (K) values of complexes (**1-3**) determined from CV using equation 7 are in order of (**3)** > (**2)** > (**1)** and were found to be similar to the values obtained from UV-visible spectroscopy (Table 3). The occurrence of a stretched aromatic system in complex **3** helped it binding more firmly to SS-DNA bases hence have a higher K value than complex **2**. Butyl moiety can form extra hydrophobic interactions with the nucleotide bases hence have higher binding constant than complex **1.**[20]

The binding site size (n) of SS-DNA's, with which complexes (**1-3**) interact is calculated by using equation 8 (Table 4).[45]

$$C_b/C_f = K[DNA]/2s \quad (8)$$

Where, s is the number of binding sites [or concentration of base pairs]. The binding size for all complexes (**1-3**)-DNA found to be greater than **1**, however the binding site's size data showed that complex **3** interacts with more base pairs of the SS-DNA than other complexes.

TABLE 4 Cyclic voltammetry parameters of organotin (IV) complexes (**1-4)**

Sample	**Do** **(cm^2s^{-1})**	**K** **(M^{-1})**	**s** **(bp)**	**ΔG** **(kJ/mol)**
1	3.19E-10			
1+DNA	1.47E-10	1.60E+04	0.47	-23.97
2	4.51E-10			
2+DNA	1.16E-10	6.36E+04	1.64	-27.40
3	8.33E-10			
3+DNA	1.15E-10	6.53E+04	1.45	-27.46

Differential pulse voltammetry

The DPV of complexes (**1-3**) was done (Figure 8). DNA interaction studies with DPV with and without addition of SS-DNA was also done. Without the existence of SS-DNA, the peak potential (E/V) values were observed at -1.46, -1.36, -1.30 and the peak current (μA) value -0.27, -0.29 and -0.27 for complexes (**1-3**), respectively. The Peak potential (E) value are in accordance with CV studies. In DPV, the $W^{1/2}$ value for all organotin (IV) complexes (**1-3**) are approximately equal to

200 mV, which suggest a 2e transfer process as observed in CV. In presence of SS-DNA (100 μM) in the solution, the voltammogram (DPV) of diorganotin(IV) complex **1**-**3**, showed a decrease in peak intensity 48%, 22% and 26%, as well as a shift to a more negative potential, -1.51 V, -1.38 V, -1.31 V was observed similar to the CV data. Intercalative mode of interaction was also observed from above results.[23,46]

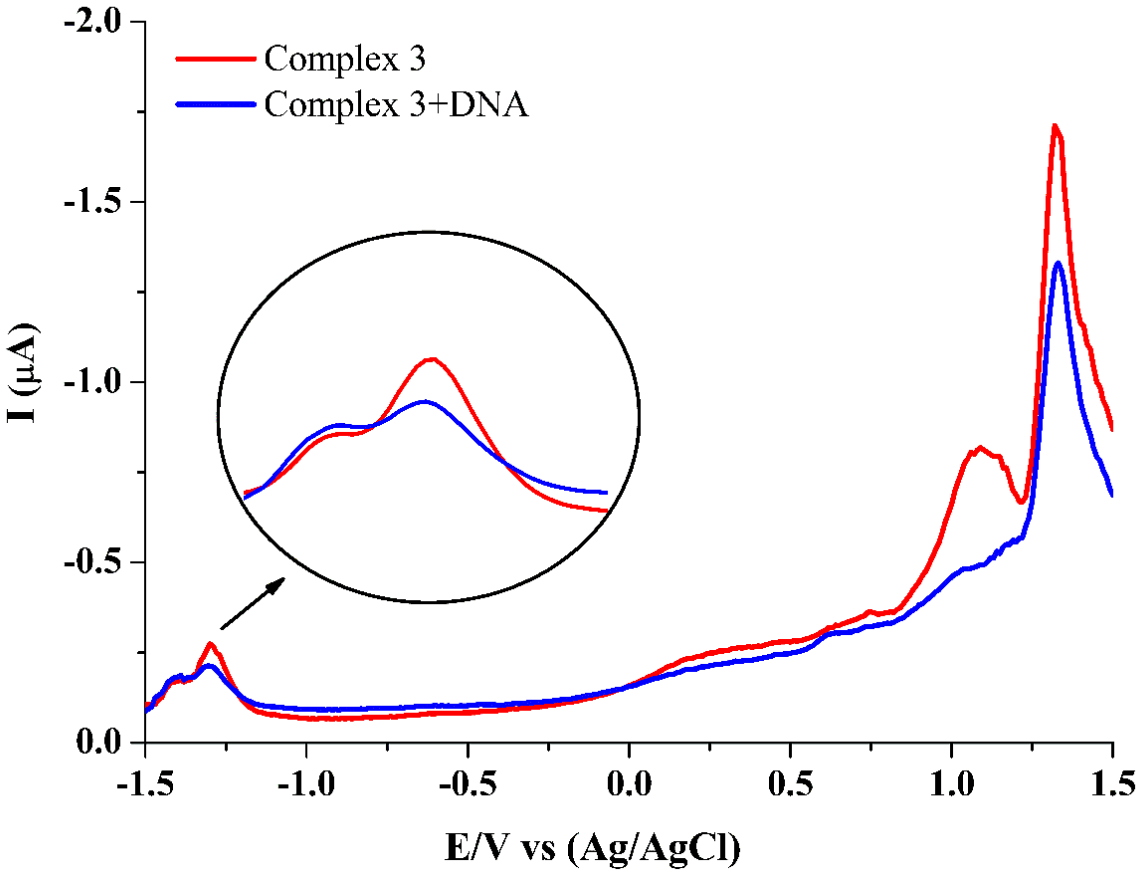

FIGURE 8 Differential pulse voltammograms of complex **3** in the absence (--) and presence (--) of (100 μM) SS-DNA.

Square Wave Voltammetry

The free Complexes **1–3** exhibits reduction peak potential (E/V) at -1.46, -1.36, -1.31 and peak current (μA) values at 0.12, 0.24 and 0.14, respectively (Figure 9). After addition of 100 μM SS-DNA to complex (**1-3**) solution of 3 mM concentration, changes in the potential and current of reduction peak are detected. The (E) peak potential is shifted to more negative values (-1.51, -

1.38, -1.36) and total shift of 50 mV, 20 mV and 40 mV is observed, for complexes (**1-3**), respectively. The peak current (I) decline, on adding of SS-DNA due to the binding of complexes and % decrease observed in its value is 39, 42, 52, for complexes (**1-3**), respectively. The decline in peak current (I) value in addition to shift in peak potential (E), is a typical indication of the intercalation mode of drug-DNA interaction.[44,47]

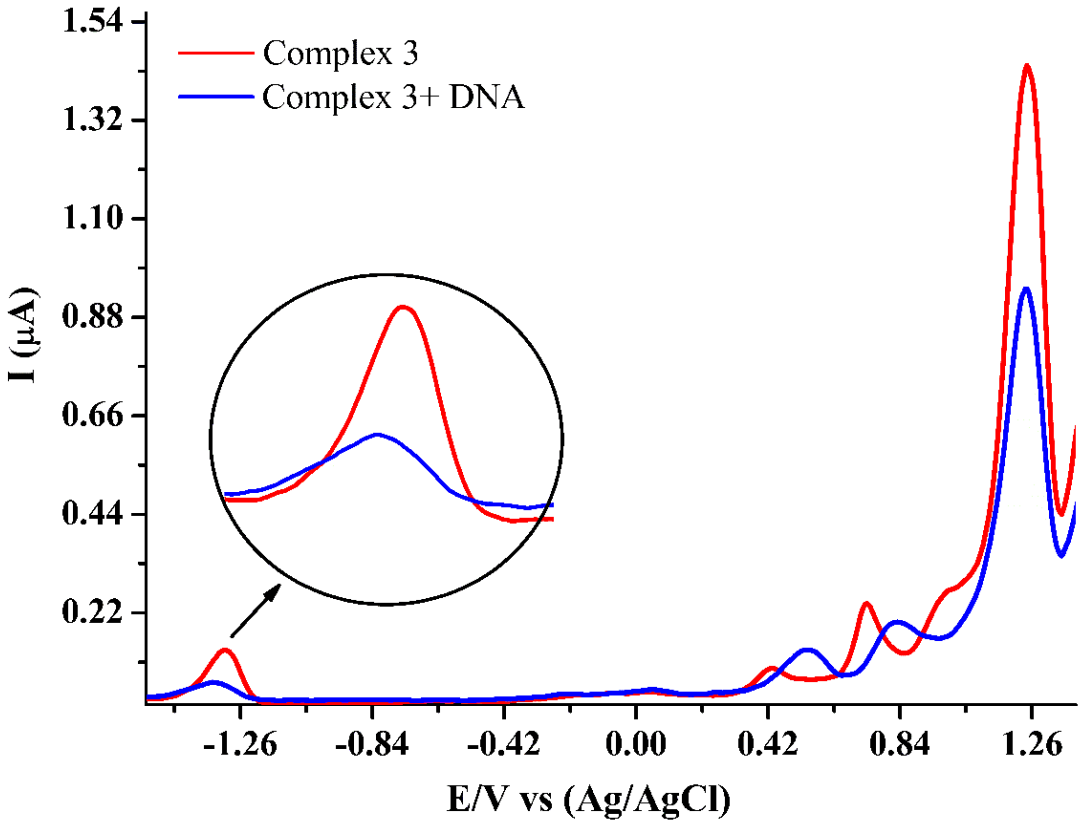

FIGURE 9 Square Wave voltammograms of complex **3** in the absence (--) and presence (--) of (100 μM) SS-DNA.

3.5. Docking analysis

To find the binding mode of the newly synthesized compounds with SS-DNA, molecular docking was performed and the results are shown in Table 5 and Figure 10. The docking results have shown a mixed binding mode consisting partial intercalation and groove binding of the compounds with SS-DNA. Among the synthesized complexes strongest interaction was shown by the complex **3** with a docking score of -8.12. The complex **3** has shown three hydrogen bond donors, one H- pi,

and two pi-H interactions with DG2, DG2, DT19, DC1, DC3 and DT19 active residues as presented in Figure 10a. The complex **4** with a docking score -8.10 has shown two H-donor, one H-pi and one pi-H polar interactions with the active residues DA5, DA17, DC3 and DA18 of DNA, respectively as shown in Figure 10b. The complex **2** with a docking score -7.38 has developed two H-donor, one H-acceptor and one pi-H interactions with DG4, DG4, DA5 and DT20 active residues of DNA, respectively as presented in Figure 10c. The complex (**1)** (docking score -7.27) developed two Hydrogen donor interactions with DA5 and DA17 interacting residues of DNA, one H-pi with DG16 and one pi-H with DG4 as shown in Figure 10d. The free ligand **H_2L** with a lowest docking score of -5.27 has shown one hydrogen acceptor and one H-donor interaction with DC3, DC3 active residues of DNA as shown in Figure 10e. The data obtained for DNA interaction studies from theoretical calculation via docking studies matches well with that observed from spectroscopic and electrochemical analysis.

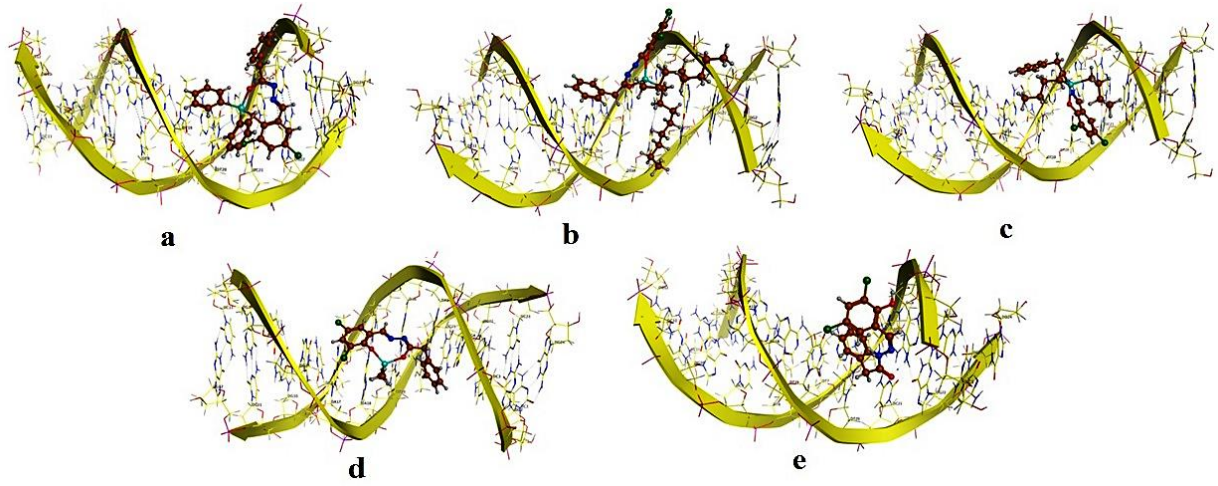

FIGURE 10 Molecular docked model of complexes **3** (a), **4** (b), **2** (c), **1** (d) and **H_2L** (e) with DNA (PDB 1D:1BNA)

TABLE 5 DNA Interaction report of ligand (**H_2L**) and complexes (**1-4**)

Code	Ligand	Receptor	Residue	Interaction	Distance	E	Docking score
H_2L	O14	OP2	DC3	(A)H-donor	2.89	-1.9	-5.27
	O17	N4	DC3	(A)H-acceptor	3.08	-0.7	
1	C16	N7	DA5	(A)H-donor	3.61	-0.2	-7.27
	CL40	OP2	DA17	(B)H-donor	3.52	-1.6	
	C2	5-ring	DG16	(B)H-pi	4.53	-0.4	
	6-ring	C2'	DG4	(A)pi-H	4.75	-0.2	
2	C7	O6	DG4	(A)H-donor	3.45	-0.2	-7.38
	C9	O6	DG4	(A)H-donor	3.44	-0.2	
	N11	N6	DA5	(A)H-acceptor	3.15	-2.1	
	6-ring	C7	DT20	(B)pi-H	4.40	-0.2	
3	C9	N7	DG2	(A)H-donor	3.32	-0.3	-8.12
	C16	OP2	DG2	(A)H-donor	3.14	-0.2	
	C47	OP2	DT19	(B)H-donor	3.17	-0.2	
	C7	6-ring	DC1	(A)H-pi	4.63	-0.3	
	6-ring	C5	DC3	(A)pi-H	4.43	-0.4	
	6-ring	C2'	DT19	(B)pi-H	4.40	-0.2	
4	C7	OP2	DA5	(A)H-donor	3.60	-0.2	-8.10
	C24	OP2	DA17	(B)H-donor	3.75	-0.2	
	C46	6-ring	DC3	(A)H-pi	4.43	-0.2	
	6-ring	N6	DA18	(B)pi-H	4.75	-0.3	

3.6. Antioxidant assay

Antioxidant activity is frequently measured using DPPH, a purple-coloured stable free radical that transforms into a diamagnetic molecule by receiving hydrogen radical or an electron from test compounds, resulting in a colour change and a drop in absorbance of 517 nm.[48-49] The synthesized ligand (**H_2L**) its complexes (**1-4**) have been investigated for their antioxidant ability against DPPH. The results showed that when concentration of test compounds was increased, its antioxidant activity also increased, as evident from Figure 11. The % scavenging activity of ligand **H_2L** obtained is 51% where its value increases due to complex formation upto 74% at 200 μg/mL concentration and this might be related to the fact that there are more atoms available for hydrogen abstraction up on complexation. The IC_{50} values were calculated for the ligand and complexes (**1-4**), the value obtained for ligand **H_2L** is 172 μg/mL. The ligand showed antioxidant activity due to the hydrogen removal from hydoxyl group, which reacts with the DPPH radical to generate a

stable molecule.[43] The antioxidant activity increased due to complexation and the IC_{50} values for the complexes (**1–4**) varied between 27 and 79 µg/mL (Table 6). The abstraction of azomethane hydrogen becomes easy upon complexation due to its more acidic nature.[26] A potential exchanging method involves the donation of a proton from the ligand, which stabilises the charge throughout the complex and alters its capacity for charge delocalization.The order of antioxidant activity in synthesized compounds was **2** > **3** > **1**> **4** > **H_2L**. The higher antioxidant activity of complex **2** could be due to presence of butyl groups which are electron donating and similarly for complex **3** high antioxidant activity is due to phenyl ring's role in the donation of electron, making it more effective antioxidant agents.

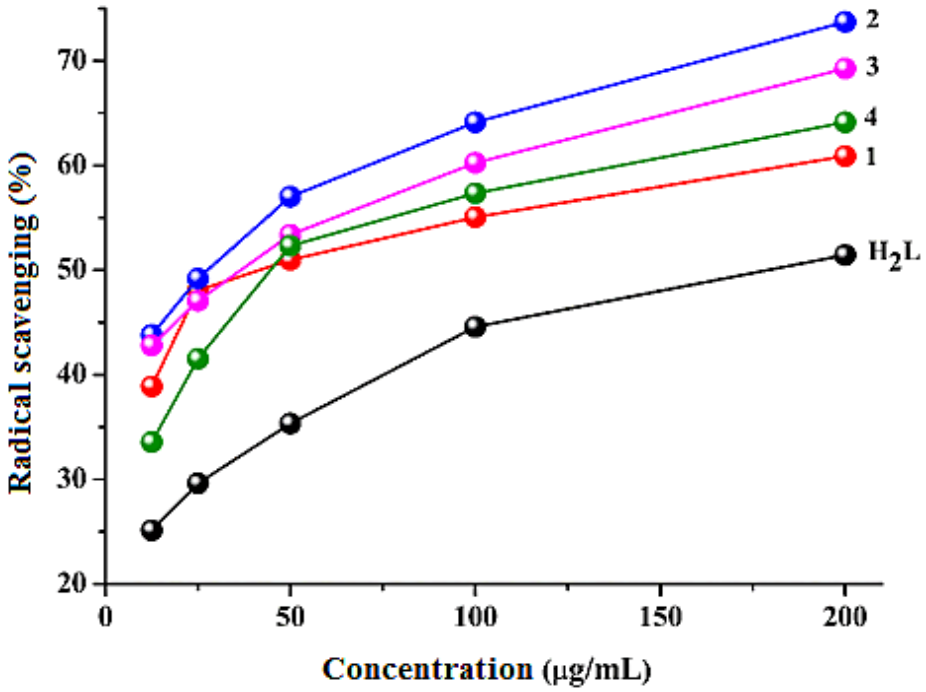

FIGURE 11 DPPH radical scavenging activity of ligand (**H_2L**) and complexes (**1-4**)

TABLE 6 Antioxidant activity of ligand (**H_2L**) and complexes (**1-4**)

Compounds	**IC_{50} μg/mL**
H_2L	172
1	69
2	27
3	44
4	79
Ascorbic acid	14

4. CONCLUSIONS

Four new diorganotin(IV) complexes of N'-(3,5-dichloro-2-hydroxybenzylidene)-2-phenylacetohydrazide **H_2L** were synthesized and characterized by IR spectrscopy, mass spectrometery, NMR (^1H and ^{13}C) spectroscopy and single crystal X-ray analysis. The pentagonal geometry of complexes (**1-4**) was indicated by the spectroscopic analysis and the molecular structure of complex (**1**) was found to be distorted towards square pyramidal geometry. The DNA-interaction studies via experimental techniques: UV-visible spectroscopy, CV, DPV, SWV as well as theoretical studies (docking calculations) showed that complex (**3)** have highest binding ability with SS-DNA and the interaction is intercalative in nature. All synthesized complexes (**1-4**) were potential active antioxidants however complex **2** showed the highest DPPH antioxidant activity.

AUTHOR CONTRIBUTIONS

Shaista Ramzan: Formal analysis; Investigation; Validation; Writing – original draft. **Shahnaz Rahim:** Software. **Tasleem Hussain:** Writing – review & editing. **Katherine H. Holt:** Methodology; Supervision. **Jeremy Karl Cockcroft:** Investigation. **Niaz Muhammad:** Formal analysis; Writing – review & editing. **Zia Ur-Rehman:** Writing – review & editing. **Asif Nawaz:**

Investigation. **Shaukat Shujah:** Conceptualization; Methodology; Resources; Supervision; Writing – review & editing.

ACKNOWLEDGEMENTS

The authors Shaista Ramzan and Shaukat Shujah are thankful to HEC Pakistan for financial support under the PhD Indigenous Fellowship Program, [Phase-II, Batch-III, PIN Code: 315-9545-2PS3-074] and HEC IRSIP (PIN Code: IRSIP 45 PSc 05).

CONFLICT OF INTEREST

The authors declare that they have no known competing financial interests or personal relationships that could have appeared to influence the work reported in this paper.

DATA AVAILIBILITY STATEMENT

Crystallographic data for the structure of complex **1** in this paper have been deposited with the Cambridge Crystallographic Data Centre, CCDC, 12 Union Road, Cambridge CB21EZ, UK. Copies of the data can be obtained free of charge on quoting the depository numbers CCDC-2238037 for complex **1.** (Fax: +44-1223-336-033; E-Mail: deposit@ccdc.cam.ac.uk, http://www.ccdc.cam.ac.uk). Spectroscopic data are available as supplementary material.

ORCID

Shaista Ramzan https://orcid.org/0000-0001-5889-9715

Shahnaz Rahim https://orcid.org/0009-0006-2793-7735

Tasleem Hussain https://orcid.org/0000-0003-3293-7546

Katherine H. Holt https://orcid.org/0000-0002-3644-1663

Jeremy Karl Cockcroft https://orcid.org/0000-0002-4954-651X

Niaz Muhammad https://orcid.org/0000-0001-8431-192X

Zia Ur-Rehman https://orcid.org/0000-0002-1436-3131

Asif Nawaz https://orcid.org/0009-0005-0529-2350

Shaukat Shujah https://orcid.org/0000-0001-6605-179X

REFERENCES

[1] M. Roy, S. Roy, K.S. Singh, J. Kalita, S.S. Singh, *Inorganica Chim. Acta*, **2016,** 439, 164-172.

[2] E.A. Nikitin, D.B. Shpakovsky, V.Y. Tyurin, A.A. Kazak, Y.A. Gracheva, V.A. Vasilichin, M.S. Pavlyukov, E.M. Mironova, V.E. Gontcharenko, K.A. Lyssenko, A.A. Antonets, L.G. Dubova, P.N. Shevtsov, E.F. Shevtsova, M.A. Shamraeva, A.A. Shtil, E.R. Milaeva, *J. Organomet. Chem.*, **2022**, 959, 122212.

[3] T.A. Antonenko, Y.A. Gracheva, D.B. Shpakovsky, M.A. Vorobyev, V.A. Tafeenko, D.M. Mazur, E.R. Milaeva, *J. Organomet. Chem.*, **2022**, 960, 122191.

[4] M. Dahmani, T. Harit, A. Et-touhami, A. Yahyi, D. Eddike, M. Tillard, R. Benabbes, *J. Organomet. Chem.*, **2021**, 948, 121913.

[5] R. Zafar, K. Shahid, L.D. Wilson, M. Fahid, M. Sartaj, W. Waseem, M. Saeed Jan, M. Zubair, A. Irfan, S. Ullah, A. Sadiq, *J. Biomol. Struct. Dyn.*, **2021**, 8, 1-11.

[6] K. Gholivand, A.A. EbrahimiValmoozi, A. Gholami, M. Dusek, V. Eigner, S. Abolghasemi, *J. Organomet. Chem.*, **2016**, 806, 33-44.

[7] M.A. Girasolo, A. Attanzio, P. Sabatino, L. Tesoriere, S. Rubino, G. Stocco, *Inorganica Chim. Acta*, **2014**, 423, 168-176.

[8] H. Hu, J. Pang, P. Gong, L. Chen, J. Zhao, *Inorg. Chem.* **2020**, 59, 11287-11297.

[9] T. Drake, P. Ji, W. Lin, *Acc. Chem. Res.*, **2018**, 51, 2129-2138.

[10] M. Sirajuddin, S. Ali, A. Badshah, *J. Photochem. Photobiol. B, Biol.*, **2013,** 124, 1-19.

[11] Y. Zhou, Y. Li, *Biophys. Chem.*, **2004**, 107, 273-281.

[12] Y. Ni, D. Lin, S. Kokot, *Talanta*, **2005**, 65, 1295-1302.

[13] H. Li, W. Mei, Z. Xu, D. Pang, L. Ji, Z. Lin, *J. Electroanal. Chem.* **2007**, 600, 243-250.

[14] L.H. Guo, X.Q. Yang, *Analyst*, **2005**, 130, 1027-1031.

[15] A.M. Abu-Dief, L.H. Abdel-Rahman, E.F. Newair, N.A. Hashem, J Sohag, *J. Sci.,* **2021,** 6, 9-25.

[16] R. Mehandi, R. Arif, M. Rana, S. Ahmedi, R. Sultana, M.S. Khan, M. Maseet, M. Khanuja, N. Manzoor, Rahisuddin, N. Nishat, *J. Mol. Struct.,* **2021,** 1245, 131248.

[17] G. Zhang, X. Hu, J. Pan, *Spectrochim. Acta A Mol. Biomol. Spectrosc.,* **2011**, 78, 687-694.

[18] X. Ling, W. Zhong, Q. Huang, K. Ni, *J. Photochem. Photobiol. B, Biol.*, **2008**, 93, 172-176.

[19] S. Shujah, S. Ali, N. Khalid, N. Muhammad, A. Meetsma, A. Wadood, H. Khan, *Polyhedron*, **2022**, 215, 115678.

[20] S. Shujah, A. Shah, Z. Rehman, N. Muhammad, R. Qureshi, A.N. Khalid, A. Meetsma, *Eur. J. Med. Chem.,* **2010**, 45, 2902-2911.

[21] M. Tariq, R. Khan, A. Hussain, A. Batool, F. Rasool, M. Yar, K. Ayub, M. Sirajuddin, F. Ullah, S. Ali, A. Akhtar, S. Kausar, A.A. Altaf, *J Coord Chem.,* **2021**, 74, 2407-2426.

[22] M. Sirajuddin, S. Ali, F.A. Shah, M. Ahmad, M.N. Tahir, *J. Iran. Chem. Soc.,* **2014**, 11, 297-313.

[23] N. Uddin, F. Rashid, S. Ali, S.A. Tirmizi, I. Ahmad, S. Zaib, M. Zubair, P.L. Diaconescu, M.N. Tahir, J. Iqbal, *J. Biomol. Struct. Dyn.*, **2020**, 38, 3246-3259.

[24] A. Braca, N. De Tommasi, L. Di Bari, C. Pizza, M. Politi, I. Morelli, *J. Nat. Prod.,* **2001,** 64, 892-895.

[25] B. Bozin, N. Mimica-Dukic, I. Samojlik, A. Goran, R. Igic, *Food chem., **2008***, 111, 925-929.

[26] J. Devi, J. Yadav, N. Singh, *Res. Chem. Intermed.*, **2019**, 45, 3943-3968.

[27] H.L. Singh, J.B. Singh, S. Bhanuka, *Res. Chem. Intermed***., 2016**, 42, 997-1015.

[28] S. Shujah, N. Khalid, S. Ali, *Russ. J. Gen. Chem.,* **2017**, 87, 515-522.

[29] S. Shujah, S. Ali, N. Khalid, M.J. Alam, S. Ahmad, A. Meetsma, *Chem. Pap.*, **2018,** 72, 903-919.

[30] T.P. Lockhart, W.F. Manders, *Inorg. Chem.,* **1986**, 25, 892-895.

[31] T.P. Lockhart, W.F. Manders, *J. Am. Chem. Soc.*, **1987,** 109, 7015-7020.

[32] B.Z. Momeni, V. Noroozi, *Monatsh. Chem.*, **2017**, 148, 893-900.

[33] M. Sirajuddin, V. McKee, M. Tariq, S. Ali, *Eur. J. Med. Chem.*, **2018**, 143, 1903-1918.

[34] M. Nath, M. Vats, P. Roy, *Chemistry for Sustainable Development*, Springer Netherlands, Dordrecht, **2012**

[35] K.W. Kohn, M.J. Waring, D. Glaubiger, C.A. Friedman, *Cancer Res.*, **1975**, 35, 71-76.

[36] I.D. Kuntz, F.P. Gasparro, M.D. Johnston, R.P. Taylor, *J. Am. Chem. Soc.*, **1968**, 90, 4778-4781.

[37] N. Arshad, S.I. Farooqi, M.H. Bhatti, S. Saleem, B. Mirza, *J. Photochem. Photobiol. B, Biol.*, **2013**, 125, 70-82.

[38] P.D. Ross, Subramanian, *Biochemistry*, **1981**, 20, 3096-3102.

[39] M. Imran, R. Zia, T. Kondratyuk, F. Bélanger-Gariepy, *Inorg. Chem. Commun.*, **2019**, 103, 12-20.

[41] A. Ševčík, *Collect. Czechoslov. Chem. Commun.*, **1948**, 13, 349-377.

[42] J.E. Randles, *J. Chem. Soc. Faraday Trans.*, **1948**, 44, 322-327.

[43] N. Arshad, M.H. Bhatti, S.I. Farooqi, S. Saleem, B. Mirza, *Arab. J. Chem.*, **2016**, 9, 451-462.

[44] M. Shabbir, Z. Akhter, I. Ahmad, S. Ahmed, V. McKee, H. Ismail, B. Mirza, *Polyhedron*, **2017**, 124, 117-124.

[45] M.T. Carter, M. Rodriguez, A.J. Bard, *J. Am. Chem. Soc.*, **1989,** 111, 8901-8911.

[46] L. Wang, L. Lin, B. Ye, *J Pharm Biomed Anal.*, **2006**, 42, 625-629.

[47] M. Aslanoglu, G. Ayne, *Anal. Bioanal. Chem.*, **2004**, 380, 658-663.

[48] D.B. Shpakovsky, C.N. Banti, E.M. Mukhatova, Y.A. Gracheva, V.P. Osipova, N.T. Berberova, D.V. Albov, T.A. Antonenko, L.A. Aslanov, E.R. Milaeva, S.K. Hadjikakou, *J. Chem. Soc., Dalton trans.*, **2014**, 43, 6880-6890.

[49] S. Jabbar, I. Shahzadi, R. Rehman, H. Iqbal, Qurat-Ul-Ain, A. Jamil, R. Kousar, S. Ali, S. Shahzadi, M.A. Choudhary, *J Coord Chem.*, **2012**, 65, 572-590.

TABLE 1 Structural parameters and crystal data for complex (**1**)

Parameters	**Complex 1**
Empirical formula	$C_{17}H_{16}Cl_2N_2O_2Sn$
Formula weight	469.91
Crystal system	Monoclinic

Space group	$P2_1/c$
a (Å)	9.0129(3)
b (Å)	10.1263(3)
c (Å)	19.8558(7)
α (°)	90
β (°)	89.860(3)
γ (°)	90
Volume ($Å^3$)	1812.18(10)
Z	4
Crystal habit	Block
Crystal size/mm^3	0.331 × 0.168 × 0.162
Temperature/K	150
P (g/cm^3)	1.722
μ ($mm^{-1)}$	1.716
F(000)	928
Radiation	MoKα (λ = 0.71073)
2Θ range for data collection/°	7.306 to 59.144
Index ranges	$-11 \leq h \leq 12$, $-13 \leq k \leq 14$, $-25 \leq l \leq 26$
Reflections collected	30600
Independent reflections	4720 [R_{int} = 0.0367, R_{sigma} = 0.0262]
Data/restraints/parameters	4720/15/277
Goodness-of-fit on F^2	1.059
Final R indexes [I>=2σ (I)]	R_1 = 0.0276, wR_2 = 0.0596
Final R indexes [all data]	R_1 = 0.0352, wR_2 = 0.0632
Largest diff. peak/hole (e $Å^{-3}$)	0.52/-0.70

TABLE 2 Selected bond lengths (Å) and bond angles (˚) of Complex (**1**)

Bond lengths of Complex 1			
Sn(1)-O(1)	2.0927(16)	N(1)-N(2)	1.404(3)
Sn(1)-O(2)	2.1428(16)	N(2)-C(8)	1.304(3)
Sn(1)-N(1)	2.1782(18)	N(1)-C(7)	1.294(3)

Sn(1)-C(9)	2.099(3)	C(1)-O(1)	1.310(3)
Sn(1)-C(10)	2.094(3)	C(1)-O(8)	1.286(3)
Bond Angles of Complex 1			
O(1)-Sn(1)-O(2)	154.87(7)	O(2)-Sn(1)-C(10)	94.06(11)
O(1)-Sn(1)-N(1)	82.37(7)	O(2)-Sn(1)-C(9)	94.69(9)
O(1)-Sn(1)-C(9)	97.47(10)	N(1)-Sn(1)-C(9)	113.30(9)
O(1)-Sn(1)-C(10)	94.06(11)	N(1)-Sn(1)-C(10)	115.17(10)
O(2)-Sn(1)-N(1)	72.62(6)	C(10)-Sn(1)-C(9)	131.21(12)
C(8)-N(2)-N(1)	110.72(18)		

TABLE 3 Thermodynamic data and binding constants of ligand (**H_2L)** and its complexes (**1-4**)

Compounds	**T (K)**	**K_b**	**ΔG (kJ/mol)**	**ΔH (kJ)**	**ΔS (kJ/K)**
H_2L	298	1.06E+04	-22.96	24.26	0.16
	310	1.55E+04	-24.87		
1	298	1.30E+04	-23.48	59.69	0.28

	310	6.56E+03	-26.82		
2	298	6.28E+04	-27.37	7.53	0.12
	310	7.20E+03	-28.78		
3	298	1.93E+05	-30.15	9.99	0.13
	310	2.25E+05	-31.77		
4	298	2.35E+04	-24.93	23.06	0.16
	310	3.37E+04	-26.87		

TABLE 4 Cyclic voltammetry parameters of organotin (IV) complexes (**1-4)**

Sample	Do (cm^2s^{-1})	K (M^{-1})	s (bp)	ΔG (kJ/mol)
1	3.19E-10			
1+DNA	1.47E-10	1.60E+04	0.47	-23.97
2	4.51E-10			
2+DNA	1.16E-10	6.36E+04	1.64	-27.40
3	8.33E-10			
3+DNA	1.15E-10	6.53E+04	1.45	-27.46

TABLE 5 DNA Interaction report of ligand (**H_2L**) and complexes (**1-4**)

Code	Ligand	Receptor	Residue	Interaction	Distance	E	Docking score
H_2L	O14	OP2	DC3	(A)H-donor	2.89	-1.9	-5.27
	O17	N4	DC3	(A)H-acceptor	3.08	-0.7	
1	C16	N7	DA5	(A)H-donor	3.61	-0.2	-7.27
	CL40	OP2	DA17	(B)H-donor	3.52	-1.6	
	C2	5-ring	DG16	(B)H-pi	4.53	-0.4	
	6-ring	C2'	DG4	(A)pi-H	4.75	-0.2	
2	C7	O6	DG4	(A)H-donor	3.45	-0.2	-7.38
	C9	O6	DG4	(A)H-donor	3.44	-0.2	
	N11	N6	DA5	(A)H-acceptor	3.15	-2.1	
	6-ring	C7	DT20	(B)pi-H	4.40	-0.2	
3	C9	N7	DG2	(A)H-donor	3.32	-0.3	-8.12
	C16	OP2	DG2	(A)H-donor	3.14	-0.2	
	C47	OP2	DT19	(B)H-donor	3.17	-0.2	
	C7	6-ring	DC1	(A)H-pi	4.63	-0.3	
	6-ring	C5	DC3	(A)pi-H	4.43	-0.4	
	6-ring	C2'	DT19	(B)pi-H	4.40	-0.2	
4	C7	OP2	DA5	(A)H-donor	3.60	-0.2	-8.10
	C24	OP2	DA17	(B)H-donor	3.75	-0.2	
	C46	6-ring	DC3	(A)H-pi	4.43	-0.2	
	6-ring	N6	DA18	(B)pi-H	4.75	-0.3	

TABLE 6 Antioxidant activity of ligand (**H_2L**) and complexes (**1-4**)

Compounds	IC_{50} μg/mL
H_2L	172
1	69
2	27
3	44
4	79
Ascorbic acid	14